Genomic Analysis of the Clonal Origins of Relapsed Acute Lymphoblastic Leukemia

Charles G. Mullighan, *et al.*

Science **322**, 1377 (2008);
DOI: 10.1126/science.1164266

Aqueous calcium concentrations are already either below or near experimentally defined thresholds of population fitness for calcium-rich crustacean zooplankton in a large proportion of lakes on the southeastern Canadian Shield, and additional declines are predicted for the next half century (*29*). The declining calcium trend we have observed is not restricted to Ontario; similar patterns have been observed in many other softwater regions of Europe and North America (*1*–*3*, *30*). Thus, we predict a similar threat to the abundances of calcium-rich zooplankton in other lake districts with historically high acid-deposition rates. Calcium-rich daphniids are some of the most abundant zooplankton in many lake systems, and their loss will substantially affect food webs. Furthermore, it is likely that the calcium decline will influence other aquatic biota, not just daphniids. The ecological effects may transcend aquatic boundaries to affect a variety of calcium-rich biota.

References and Notes

1. J. L. Stoddard *et al*., *Nature* **401**, 575 (1999).
2. S. A. Watmough, J. Aherne, P. J. Dillon, *Can. J. Fish. Aquat. Sci.* **60**, 1095 (2003).
3. B. L. Skjelkvåle *et al*., *Environ. Pollut.* **137**, 165 (2005).
4. S. A. Norton, J. Veselý, in *Treatise on Geochemistry*, vol. 9, H. D. Holland, K. K. Turekian, Eds. (Elsevier-Pergamon, Oxford, 2003), pp. 367–406.
5. D. Houle, R. Ouimet, S. Couture, C. Gagnon, *Can. J. Fish. Aquat. Sci.* **63**, 471 (2006).
6. J. W. Kirchner, E. Lydersen, *Environ. Sci. Technol.* **29**, 1953 (1995).
7. G. E. Likens, C. T. Driscoll, D. C. Buso, *Science* **272**, 244 (1996).
8. T. G. Huntington *et al*., *Soil Sci. Soc. Am. J.* **64**, 1845 (2000).
9. S. A. Watmough *et al*., *Environ. Monit. Assess.* **109**, 1 (2005).
10. D. Ashforth, N. D. Yan, *Limnol. Oceanogr.* **53**, 420 (2008).
11. J. P. Smol, *Pollution of Lakes and Rivers: A Paleoenvironmental Perspective* (Blackwell, Oxford, ed. 2, 2008).
12. M. A. Leibold, *Am. Nat.* **134**, 922 (1989).
13. H. Cyr, J. M. Curtis, *Oecologia* **118**, 306 (1999).
14. A. Jeziorski, N. D. Yan, *Can. J. Fish. Aquat. Sci.* **63**, 1007 (2006).
15. W. Keller, S. S. Dixit, J. Heneberry, *Can. J. Fish. Aquat. Sci.* **58**, 2011 (2001).
16. A. Korhola, M. Rautio, in *Tracking Environmental Change Using Lake Sediments*, vol. 4, J. P. Smol, H. J. B. Birks, W. M. Last, Eds. (Kluwer Academic, Dordrecht, Netherlands, 2001), pp. 4–41.
17. R. W. Battarbee, D. F. Charles, S. S. Dixit, I. Renberg, in *The Diatoms: Applications for the Environmental and Earth Sciences*, E. F. Stoermer, J. P. Smol, Eds. (Cambridge Univ. Press, Cambridge, 1999), pp. 85–127.
18. R. I. Hall, J. P. Smol, *Can. J. Fish. Aquat. Sci.* **53**, 1 (1996).
19. A. M. DeSellas, A. M. Paterson, J. N. Sweetman, J. P. Smol, *Hydrobiologia* **600**, 105 (2008).
20. B. K. Ginn, B. F. Cumming, J. P. Smol, *Can. J. Fish. Aquat. Sci.* **64**, 1043 (2007).
21. T. A. Clair, T. Pollock, G. Brun, A. Ouellet, D. Lockerbie, *Environment Canada's Acid Precipitation Monitoring Networks in Atlantic Canada: Occasional Report No. 16* (Environment Canada, Ottawa, Canada, 2001).
22. C. Chan, thesis, Queen's University (2004).
23. D. F. Charles *et al*., *Biogeochemistry* **3**, 267 (1987).
24. C. T. Driscoll, K. M. Driscoll, K. M. Roy, M. J. Mitchell, *Environ. Sci. Technol.* **37**, 2036 (2003).
25. N. D. Yan *et al*., *Can. J. Fish. Aquat. Sci.* **65**, 862 (2008).
26. P. S. D. MacRae, D. A. Jackson, *Can. J. Fish. Aquat. Sci.* **58**, 342 (2001).
27. K. E. Havens, N. D. Yan, W. Keller, *Environ. Sci. Technol.* **27**, 1621 (1993).
28. Z. M. Gliwicz, *Nature* **343**, 638 (1990).
29. S. A. Watmough, J. Aherne, *Can. J. Fish. Aquat. Sci.* **65**, 821 (2008).
30. D. S. Jeffries, D. K. McNicol, R. C. Weeber, Eds., *2004 Canadian Acid Deposition Science Assessment. Chapter 6: Effects on Aquatic Chemistry and Biology* (Environment Canada, Ottawa, Canada, 2004).

31. This work was primarily supported by grants from the Natural Sciences and Engineering Research Council of Canada, as well as funding from the Ontario Ministry of the Environment, Environment Canada, and Fisheries and Oceans Canada. We thank the latter three agencies for the data used to develop Fig. 4. N.D.Y. thanks the School of Environmental Systems Engineering from the University of Western Australia for their support. We would also like to thank D. Schindler and S. Watmough for their valuable comments on this manuscript.

Supporting Online Material

www.sciencemag.org/cgi/content/full/322/5906/1374/DC1
SOM Text

21 August 2008; accepted 15 October 2008
10.1126/science.1164949

Genomic Analysis of the Clonal Origins of Relapsed Acute Lymphoblastic Leukemia

Charles G. Mullighan,[1] Letha A. Phillips,[1] Xiaoping Su,[1] Jing Ma,[2] Christopher B. Miller,[1] Sheila A. Shurtleff,[1] James R. Downing[1]*

Most children with acute lymphoblastic leukemia (ALL) can be cured, but the prognosis is dismal for the minority of patients who relapse after treatment. To explore the genetic basis of relapse, we performed genome-wide DNA copy number analyses on matched diagnosis and relapse samples from 61 pediatric patients with ALL. The diagnosis and relapse samples typically showed different patterns of genomic copy number abnormalities (CNAs), with the CNAs acquired at relapse preferentially affecting genes implicated in cell cycle regulation and B cell development. Most relapse samples lacked some of the CNAs present at diagnosis, which suggests that the cells responsible for relapse are ancestral to the primary leukemia cells. Backtracking studies revealed that cells corresponding to the relapse clone were often present as minor subpopulations at diagnosis. These data suggest that genomic abnormalities contributing to ALL relapse are selected for during treatment, and they point to new targets for therapeutic intervention.

Despite cure rates for pediatric ALL exceeding 80% (*1*), treatment failure remains a formidable problem. Relapsed ALL ranks as the fourth most common childhood malignancy and has an overall survival rate of only 30% (*2*, *3*). Important biological and clinical differences have been identified between diagnostic and relapsed leukemic cells, including the acquisition of new chromosomal abnormalities, gene mutations, and reduced responsiveness to chemotherapeutic agents (*4*–*7*). However, many questions remain about the molecular abnormalities responsible for relapse, as well as the relationship between the cells giving rise to the primary and recurrent leukemias in individual patients.

[1]Department of Pathology, St. Jude Children's Research Hospital, Memphis, TN 38105, USA. [2]Hartwell Center for Bioinformatics and Biotechnology, St. Jude Children's Research Hospital, Memphis, TN 38105, USA.

*To whom correspondence should be addressed. E-mail: james.downing@stjude.org

Single-nucleotide polymorphism (SNP) arrays have enabled genome-wide analyses of DNA CNAs and loss of heterozygosity (LOH) in cancer and have provided important insights into the pathogenesis of newly diagnosed ALL. We previously reported multiple recurring somatic CNAs in genes encoding transcription factors, cell cycle regulators, apoptosis mediators, lymphoid signaling molecules, and drug receptors in B-progenitor and T-lineage ALL (B-ALL and T-ALL) (*8*, *9*). To gain insights into the molecular lesions responsible for ALL relapse, we have now performed genome-wide CNA and LOH analyses on matched diagnostic and relapse bone marrow samples from 61 pediatric ALL patients (table S1). These samples included 47 B-ALL and 14 T-ALL cases (*10*). Samples were flow-sorted to ensure at least 80% tumor cell purity before DNA extraction (fig. S1). DNA copy number and LOH data were obtained using Affymetrix SNP 6.0 (47 diagnosis-relapse pairs) or 500K arrays (14 pairs). Remission bone marrow samples were also analyzed for 48 patients (table S1).

These analyses identified a mean of 10.8 somatic CNAs per B-ALL case and 7.1 CNAs per T-ALL case at diagnosis (table S4 and figs. S2 and S4). Of the B-ALL cases at diagnosis, 48.9% had CNAs in genes known to regulate B-lymphoid development, including *PAX5* ($N = 12$), *IKZF1* ($N = 12$), *EBF1* ($N = 2$), and *RAG1/2* ($N = 2$) (tables S5, S6, and S9). Deletion of *CDKN2A/B* was present in 36.2% of B-ALL and 71.4% T-ALL cases, and deletion

of *ETV6* was present in 11 B-ALL cases. We also identified novel CNAs involving *ARID2*, which encodes a member of a chromatin-remodeling complex (*11*); the cyclic adenosine monophosphate–regulated phosphoprotein *ARPP-21*; the cytokine receptor genes *IL3RA* and *CSF2RA* (fig. S3); and the Wnt/β-catenin pathway genes *CTNNB1*, *WNT9B*, and *CREBBP* (tables S5 and S6).

Although evidence for clonal evolution and/or selection at relapse has been reported (*4*, *6*, *7*, *12*–*21*), we observed a striking degree of change in the number, extent, and nature of CNAs between diagnosis and relapse in paired samples of ALL. A significant increase in the mean number of CNAs per case was observed in relapse B-ALL samples (10.8 at diagnosis versus 14.0 at relapse, $P = 0.0005$), with the majority being additional regions of deletion (6.8 deletions per case at diagnosis versus 9.2 deletions per case at relapse, $P = 0.0006$; 4.0 gains per case at diagnosis versus 4.8 gains per case at relapse, $P = 0.03$; table S4 and fig. S4). By contrast, no significant changes in lesion frequency were observed in T-ALL (table S4).

The majority (88.5%) of relapse samples harbored at least some of the CNAs present in the matched diagnosis sample, indicating a common clonal origin (table S5 and fig. S5); however, 91.8% exhibited a change in the pattern of CNAs from diagnosis to relapse (table S7). Of these, 34% acquired new CNAs, 12% showed loss of lesions present at diagnosis, and 46% both acquired new lesions and lost lesions present at diagnosis. In 11% of relapsed samples (three B-ALL and four T-ALL cases), all CNAs present at diagnosis were lost at relapse, raising the possibility that the relapse represents the emergence of a second unrelated leukemia. One case (BCR-ABL-SNP-15) retained the same translocation at relapse, indicating a common clonal origin. In four cases, lack of similarity of the patterns of deletion at immunoglobulin (Ig) and T cell antigen receptor (TCR) gene loci, or lack of deletions at these loci, suggested that relapse represented the emergence of a distinct leukemia (see below and figs. S6 and S7). For all other relapse cases (86%), analysis of Ig and TCR deletions demonstrated a clonal relationship between diagnostic and relapse samples (table S21 and fig. S6).

The genes most frequently affected by CNAs acquired at relapse were *CDKN2A/B*, *ETV6*, and regulators of B cell development (Table 1, Fig. 1, tables S8 to S18, and fig. S8). Sixteen B-ALL and two T-ALL cases acquired new CNAs of *CDKN2A/B*, 10 of which lacked *CDKN2A/B* deletions at diagnosis (Fig. 1, A and B, and tables S17 and S18). The *CDKN2A/B* deletions acquired at relapse were biallelic in 70% of cases, resulting in a complete loss of expression of all three encoded proteins: INK4A (p16), ARF (p14), and INK4B (p15). Deletion of *ETV6*, a frequent abnormality at diagnosis in *ETV6-RUNX1* B-ALL (*8*, *19*), was also common in relapsed ALL, being identified in 11 cases (10 B-ALLs and one T-ALL) with only one case *ETV6-RUNX1*–positive (fig. S8). Mutations of genes regulating B cell development are common at

Table 1. Targets of relapse-acquired CNAs in ALL, ranked in order of frequency.

Lesion		B-progenitor ALL	T-lineage ALL
Deletion	*CDKN2A*	16	2
	ETV6	10	1
	IKZF1	5	2
	NR3C1	4	0
	TCF3	3	0
	DMD	2	0
	ARPP-21	2	0
	BTLA/CD200	2	1
	RAG1/2	2	0
	IKZF2	1	1
	ADD3	1	0
	C20orf94	1	0
	TBL1XR1	1	0
	IKZF3	1	0
Gain	*MYB*	0	2
	DMD	1	0

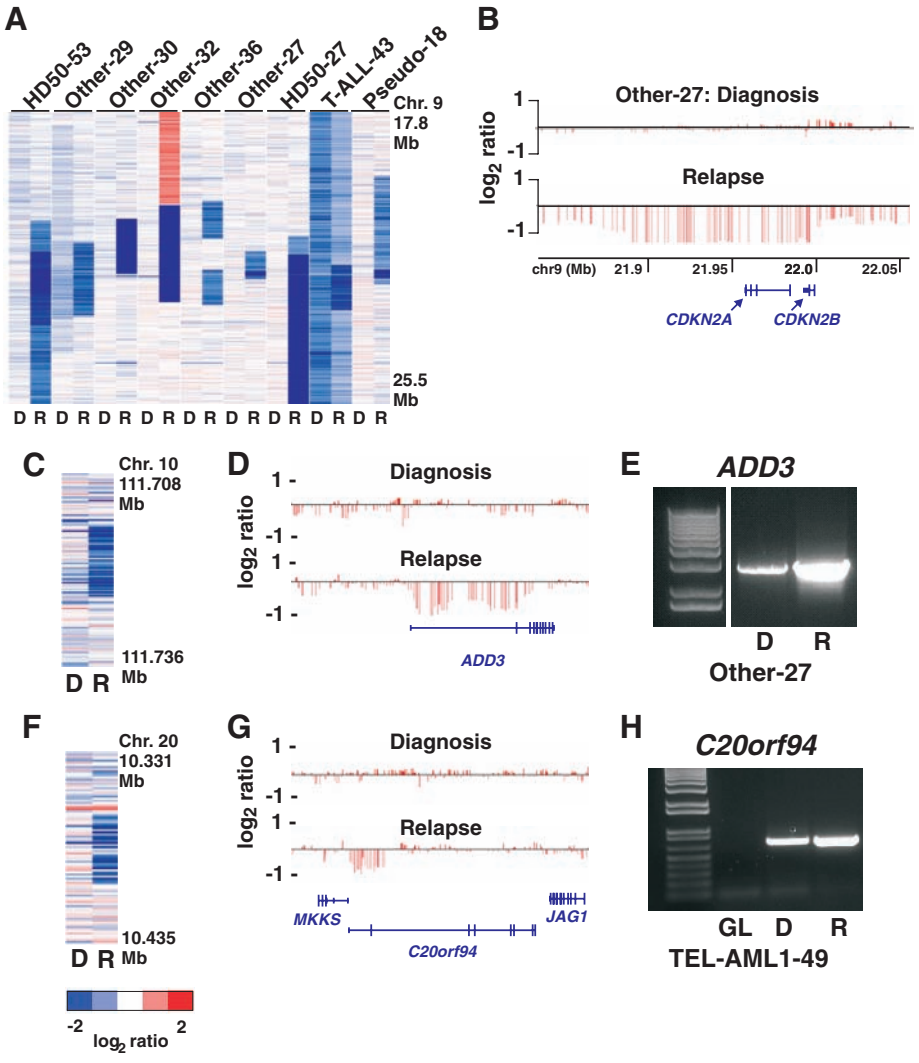

Fig. 1. Deletions of *CDKN2A/B* and lesion-specific backtracking in relapsed ALL. (**A**) Log_2 ratio Affymetrix SNP 6.0 copy number data (median smoothed with a window of five markers; blue is deletion and red is gain) of chromosome 9p flanking *CDKN2A/B* for nine representative cases showing new or more extensive deletions at this locus at relapse. Deletions in selected cases were confirmed by quantitative genomic PCR (table S17). (**B**) Coverage of the locus for one case. Each vertical red line represents the genomic position and log_2 ratio copy number of an individual marker. This case has acquired a homozygous deletion involving exon 2 of *CDKN2B* and all of *CDKN2A* at relapse. (**C** to **H**) Backtracking of CNAs by lesion-specific genomic PCR assays in ALL [(C) to (E), *ADD3*; (F) to (H), *C20orf94*]. Log_2 ratio copy number heat maps for diagnosis and relapse samples are shown in (C) and (F); genomic locations of SNP probes and regions of deletion are shown in (D) and (G). In (E) and (H), PCR for each lesion was performed for diagnosis, relapse, and (where available) germline DNA samples. In each case, a CNA-specific PCR product was observed at diagnosis as well as relapse, indicating that each CNA was present at diagnosis.

diagnosis in B-ALL (*8*), and additional lesions in this pathway were observed at relapse, with a number of cases acquiring multiple hits within the pathway (table S9). Four cases lacked CNAs in this pathway at diagnosis but acquired deletions in *PAX5* ($N = 1$), *IKZF1* ($N = 2$), or *TCF3* ($N = 1$) at relapse. Eleven cases with CNAs in this pathway at diagnosis acquired additional lesions at relapse, most commonly *IKZF1* (five cases), *IKZF2* (two cases), and *IKZF3* (one case) (figs. S9 and S10). New CNAs were also observed in *PAX5* ($N = 3$), *TCF3* ($N = 3$), *RAG1/2* ($N = 2$; figs. S9 and S10), and *EBF1* ($N = 1$; fig. S9). CNAs involving genes that encode regulators of lymphoid development were also observed in four T-ALL relapse samples, but these involved the early lymphoid regulators *IKZF1* ($N = 2$), *IKZF2* ($N = 1$), and *LEF1* ($N = 2$; table S9), rather than B lineage–specific genes such as *PAX5* and *EBF1*.

A number of other less frequent CNAs previously detected in diagnostic ALL samples (*8*) were also observed as new lesions at relapse, including CNAs of *ADD3*, *ARPP-21*, *ATM*, *BTG1*, *CD200/BTLA*, *FHIT*, *KRAS*, *IL3RA/CSF2RA*, *NF1*, *PTCH*, *TBL1XR1*, *TOX*, *WT1*, *NR3C1*, and *DMD* (table S8 and fig. S11). Progression of intrachromosomal amplification of chromosome 21, a poor prognostic marker in childhood ALL (*22*), was also observed in two B-ALL cases (fig. S12). In addition, relapsed T-ALL was remarkable for the loss and acquisition of sentinel lesions, including the loss of *NUP214-ABL1* in one case, and the acquisition of *NUP214-ABL1*, *LMO2*, and *MYB* amplification (one case each) at relapse (*8*, *23*–*25*) (table S8 and fig. S13).

In addition to defining CNAs, we performed an analysis of regions of copy-neutral LOH (CN-LOH) that can signify mutated, reduplicated genes. CN-LOH acquired at relapse was identified in only 15 B-ALL and three T-ALL cases (table S19). The most common region involved was chromosome 9p ($N = 8$), which in each case contained a homozygous *CDKN2A/B* deletion consistent with reduplication of a hemizygous *CDKN2A/B* deletion.

To determine which biologic pathways were most frequently targeted by relapse-acquired CNAs, we categorized each gene contained within altered genomic regions into one or more of 148 biologic pathways. The pathways were then assessed for their frequency of involvement by CNAs across the data set with the use of Fisher's exact test (*10*). This analysis identified cell cycle regulation and B cell development as the most common pathways targeted at relapse (table S20).

There was a clear clonal relationship between the diagnosis and relapse ALL samples in most cases (93.6% of B-ALL and 71.4% of T-ALL cases). This suggests that the relapse-associated CNAs either (i) were present at low levels at diagnosis and selected for at relapse, or (ii) were acquired as new genomic alterations after initial therapy. To explore these possibilities, we mapped the genomic breakpoints of several CNAs acquired at relapse (*ADD3*, *C20orf94*, *DMD*, *ETV6*, *IKZF2*, and *IKZF3*) and developed lesion-specific polymerase chain reaction (PCR) assays. Evidence of the relapse clone was detected in 7 of 10 diagnosis samples analyzed (Fig. 1, C to H, and figs. S14 and S15). Thus, the relapse clone is frequently present as a minor subpopulation at diagnosis.

By carefully analyzing the changes in CNAs between matched diagnostic and relapse samples, we were able to map their evolutionary relationship (Fig. 2). In a minority of cases, "relapse" is a misnomer, as no CNAs were shared by the diagnostic and relapse clones. The recurrent disease in these cases represents either a secondary leukemia or a leukemia arising from an ancestral clone that lacks any of the CNAs present in the diagnosis leukemia. In 8% of the cases, there were no differences in CNAs between the diagnostic and relapse clones, whereas in 34% of the cases, relapse represented clonal evolution of the diagnosis leukemic populations. Remarkably, in about half of the cases, the relapse clone was derived from an ancestral, prediagnosis leukemic precursor cell and not from the clone predominating at diagnosis. One illustrative case (Other-SNP-29) had two relapse-acquired deletions (*ETV6* and *DMD*), only one of which was present in the diagnostic sample as a minor clone (*ETV6*, fig. S15), indicating that these lesions were acquired at different stages of evolution of the relapse clone. This case provides unequivocal evidence of a common ancestral clone that gave rise to the major clone at diagnosis, and to a second clone that was present as a minor population at diagnosis but acquired different genetic alterations before emerging as the relapse clone.

These results complement those of previous studies examining individual genetic loci in relapsed ALL (*6*, *14*, *16*, *20*, *21*, *26*–*28*) and provide important insights into the spectrum of genetic lesions that underlie this process. Although our data are limited to a single class of mutations (CNAs), they show that no single genetic lesion or alteration of a single pathway is responsible for relapse. Moreover, global genomic instability does not appear to be a prevalent mechanism. Instead, a diversity of mutations appear to contribute to relapse, with the most common alterations targeting key regulators of tumor suppression, cell cycle control, and lymphoid/B cell development. Notably, few lesions involved genes with roles in drug import, metabolism, export, and/or response (an exception being the glucocorticoid receptor gene *NR3C1*), which suggests that the mechanism of relapse is more complex than simple "drug resistance."

The diversity of genes that are targeted by relapse-associated CNAs, coupled with the presence of the relapse clone as a minor subpopulation at diagnosis that escapes drug-induced killing, represent formidable challenges to the development of effective therapy for relapsed ALL. Nonetheless, our study has identified several common pathways that may contain rational

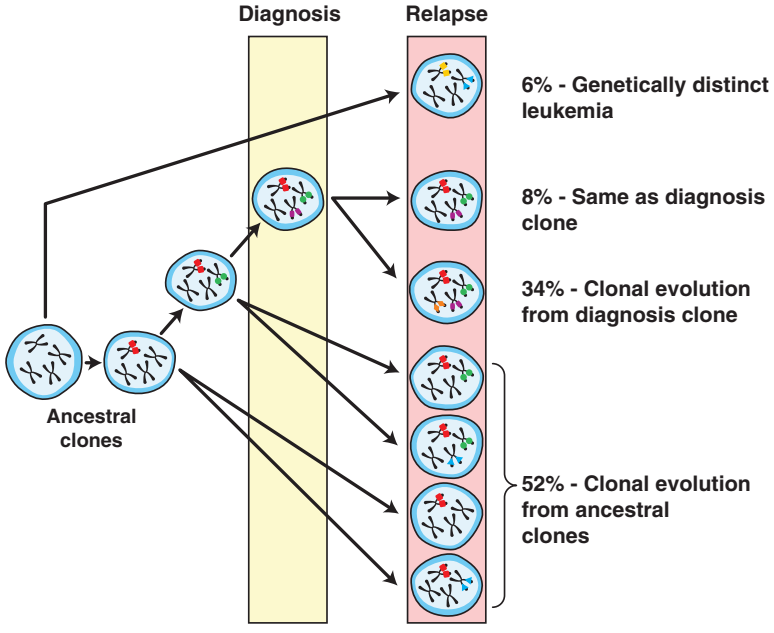

Fig. 2. Clonal relationship of diagnosis and relapse samples in ALL. The majority of relapse cases have a clear relationship to the diagnosis leukemic clone, either arising through the acquisition of additional genetic lesions or, more commonly, arising from an ancestral (prediagnosis) clone. In the latter scenario, the relapse clone acquires new lesions while retaining some but not all of the lesions found in the diagnostic sample. Lesion-specific backtracking studies revealed that in most cases the relapse clone exists as a minor subclone within the diagnostic sample before the initiation of therapy. In only a minority of ALL cases does the relapse clone represent the emergence of a genetically distinct and thus unrelated second leukemia.

targets against which novel therapeutic agents can be developed.

References and Notes

1. C. H. Pui, L. L. Robison, A. T. Look, *Lancet* **371**, 1030 (2008).
2. H. G. Einsiedel *et al.*, *J. Clin. Oncol.* **23**, 7942 (2005).
3. G. K. Rivera *et al.*, *Cancer* **103**, 368 (2005).
4. S. C. Raimondi, C. H. Pui, D. R. Head, G. K. Rivera, F. G. Behm, *Blood* **82**, 576 (1993).
5. E. Klumper *et al.*, *Blood* **86**, 3861 (1995).
6. K. W. Maloney, L. McGavran, L. F. Odom, S. P. Hunger, *Blood* **93**, 2380 (1999).
7. J. A. Irving *et al.*, *Cancer Res.* **65**, 3053 (2005).
8. C. G. Mullighan *et al.*, *Nature* **446**, 758 (2007).
9. C. G. Mullighan *et al.*, *Nature* **453**, 110 (2008).
10. See supporting material on *Science* Online.
11. Z. Yan *et al.*, *Genes Dev.* **19**, 1662 (2005).
12. J. J. Taylor *et al.*, *Leukemia* **8**, 60 (1994).
13. G. M. Marshall *et al.*, *Leukemia* **9**, 1847 (1995).
14. F. Davi, C. Gocke, S. Smith, J. Sklar, *Blood* **88**, 609 (1996).
15. R. Rosenquist *et al.*, *Eur. J. Haematol.* **63**, 171 (1999).
16. A. M. Ford *et al.*, *Blood* **98**, 558 (2001).
17. G. Germano *et al.*, *Leukemia* **17**, 1573 (2003).
18. S. Takeuchi *et al.*, *Oncogene* **22**, 6970 (2003).
19. J. Zuna *et al.*, *Clin. Cancer Res.* **10**, 5355 (2004).
20. E. R. Panzer-Grumayer *et al.*, *Clin. Cancer Res.* **11**, 7720 (2005).
21. S. Choi *et al.*, *Blood* **110**, 632 (2007).
22. A. V. Moorman *et al.*, *Blood* **109**, 2327 (2007).
23. C. Graux *et al.*, *Nat. Genet.* **36**, 1084 (2004).
24. I. Lahortiga *et al.*, *Nat. Genet.* **39**, 593 (2007).
25. E. Clappier *et al.*, *Blood* **110**, 1251 (2007).
26. A. Beishuizen *et al.*, *Blood* **83**, 2238 (1994).
27. M. Peham *et al.*, *Genes Chromosomes Cancer* **39**, 156 (2004).
28. M. Konrad *et al.*, *Blood* **101**, 3635 (2003).

29. We thank R. Ashmun and the St. Jude Flow Cytometry and Cell Sorting Shared Resource for flow sorting of leukemia samples, the St. Jude Clinical Applications Core Technology Laboratory for performing SNP arrays, L. Kiedrowski for lesion mapping and backtracking assays, and J. Stokes for assistance with artwork. Supported by the American Lebanese Syrian Associated Charities of St. Jude Children's Research Hospital and by the National Health and Medical Research Council of Australia (C.G.M.). Primary SNP array data are available from the authors upon request. J.R.D. has participated in gene expression profiling research sponsored by Roche. C.G.M. and J.R.D. have filed a patent application related to this work.

Supporting Online Material

www.sciencemag.org/cgi/content/full/322/5906/1377/DC1
Materials and Methods
SOM Text
Figs. S1 to S15
Tables S1 to S21
References

6 August 2008; accepted 27 October 2008
10.1126/science.1164266

A Genetic Framework for the Control of Cell Division and Differentiation in the Root Meristem

Raffaele Dello Ioio,[1] Kinu Nakamura,[2]* Laila Moubayidin,[1]* Serena Perilli,[1]* Masatoshi Taniguchi,[2] Miyo T. Morita,[3] Takashi Aoyama,[2] Paolo Costantino,[1] Sabrina Sabatini[1]†

Plant growth and development are sustained by meristems. Meristem activity is controlled by auxin and cytokinin, two hormones whose interactions in determining a specific developmental output are still poorly understood. By means of a comprehensive genetic and molecular analysis in *Arabidopsis*, we show that a primary cytokinin-response transcription factor, ARR1, activates the gene *SHY2/IAA3* (*SHY2*), a repressor of auxin signaling that negatively regulates the *PIN* auxin transport facilitator genes: thereby, cytokinin causes auxin redistribution, prompting cell differentiation. Conversely, auxin mediates degradation of the SHY2 protein, sustaining PIN activities and cell division. Thus, the cell differentiation and division balance necessary for controlling root meristem size and root growth is the result of the interaction between cytokinin and auxin through a simple regulatory circuit converging on the *SHY2* gene.

Postembryonic root growth is sustained by the root meristem. Stem cells in the root meristem generate transit-amplifying cells, which undergo additional division in the proximal meristem, and differentiate at the meristem transition zone that encompasses the boundary between dividing and expanding cells in the different cell files (Fig. 1A). For meristem maintenance, the rate of cell differentiation must equal the rate of generation of new cells: How this balance is achieved is a central question in plant development.

Classic plant tissue culture experiments showed that auxin and cytokinin are key signaling molecules controlling meristems activity because they antagonistically affect, in vitro, shoot and root organogenesis (*1*, *2*). Recently, the in vivo importance of the cytokinin and auxin antagonistic interaction has been proven during *Arabidopsis* root meristem size determination (*3*) and for embryonic root stem cell niche specification (*4*), but the genetic and molecular basis of this interaction remains to be clarified.

The expression domains of the genes encoding the two-component cytokinin signaling pathway, the AHK3 receptor kinase and the ARR1 and ARR12 transcription factors, and the root meristem phenotype of *ahk3*, *arr1*, and *arr12* mutants demonstrate that cytokinin acts at the transition zone to control cell differentiation rate (*3*, *5*, *6*). Furthermore, the expression patterns of cytokinin biosynthesis genes (*7*) and experiments of tissue- and spatial-specific cytokinin depletion in the root meristem showed that cytokinin specifically acts at the vascular tissue transition zone, where it controls the differentiation rate of all the other root cells by antagonizing a non–cell-autonomous signal that we suggested may be auxin (*3*). On the other hand, experiments of exogenous application of auxin and the effects of mutations in the PIN auxin efflux facilitators are consistent with a role of auxin in controlling cell division (*3*, *8*). Thus, the size of the root meristem may be established by a balance between the antagonistic effects of cytokinin, which mediates cell differentiation, and auxin, which mediates cell division.

In order to dissect the cytokinin-auxin interaction in the root meristem, we sought to identify the gene(s) immediately responsive to cytokinin signaling. Cytokinin control of root meristem size is mediated by both ARR1 and the ARR12 transcription factors, specifically expressed at the root transition zone and acting, respectively, early and late during meristem development (*3*). Whereas the root meristems of *arr12* mutants were larger than those of wild type but eventually stopped growing, *arr1* mutant meristems kept increasing in size over time (*3*). ARR1 seems therefore to have a critical role in determining root meristem size, and thus we set to verify whether this transcription factor alone would be sufficient to control cell differentiation and root meristem size. To this aim, we checked the root phenotype of plants harboring a glucocorticoid-inducible construct of ARR1 (*35S::ARR1ΔDDK:GR*) (*9*). As in the case of exogenous cytokinin applications (*3*), root meristems of *35S::ARR1ΔDDK:GR* plants were significantly reduced after 8 hours of dexamethasone (a glucocorticoid derivative) induction, suggesting that ARR1 is capable alone of controlling root meristem size (fig. S1, A and B).

The same *35S::ARR1ΔDDK:GR* construct had been previously used to identify a number of putative direct-target genes of the ARR1 transcription factor (*10*). Among the 23 putative targets of ARR1 (*10*), there is notably *SHY2*, a member of the auxin/indole-3-acetic acid inducible (*Aux/IAA*) family of genes (*11*) that act as auxin-response inhibitors by forming heterodimers with the ARF (auxin response factor) transcription factors, thereby preventing activation of auxin-responsive genes (among which are the *Aux/IAA* genes) by these latter (*12*, *13*). Auxin causes the

[1]Dipartimento di Genetica e Biologia Molecolare, Laboratorio di Genomica e proteomica funzionale dei sistemi modello (FGPL), Università La Sapienza - Piazzale Aldo Moro 5, 00185 Rome, Italy. [2]Institute for Chemical Research, Kyoto University, Uji, Kyoto 611-0011, Japan. [3]Graduate School of Biological Sciences, Nara Institute of Science and Technology, Ikoma, 630-0101, Japan.

*These authors contributed equally to this work.
†To whom correspondence should be addressed. E-mail: sabrina.sabatini@uniroma1.it